NASA Technical Paper 1069

Airflow and Thrust Calibration of an F100 Engine, S/N P680059, at Selected Flight Conditions

Thomas J. Biesiadny, Douglas Lee,
and Jose R. Rodriguez

APRIL 1978

NASA

NASA Technical Paper 1069

Airflow and Thrust Calibration of an F100 Engine, S/N P680059, at Selected Flight Conditions

Thomas J. Biesiadny, Douglas Lee,
and Jose R. Rodriguez
Lewis Research Center
Cleveland, Ohio

National Aeronautics
and Space Administration

**Scientific and Technical
Information Office**

1978

AIRFLOW AND THRUST CALIBRATION OF AN F100 ENGINE, S/N P680059, AT SELECTED FLIGHT CONDITIONS

by Thomas J. Biesiadny, Douglas Lee, and Jose R. Rodriguez
Lewis Research Center

SUMMARY

An airflow and thrust calibration of an F100 engine, S/N P680059, was conducted at the NASA Lewis Research Center in coordination with a flight test program at the NASA Dryden Flight Research Center to study airframe - propulsion-system-integration losses in turbofan-powered high-performance aircraft. The tests were conducted with and without thrust augmentation for a variety of simulated flight conditions with emphasis on the transonic regime.

The resulting corrected airflow data generalized into one curve with corrected fan speed, and corrected gross thrust increased as simulated flight conditions increased. Overall agreement between measured data and computed results from a Pratt & Whitney Aircraft in-flight thrust deck was within 1 percent for corrected airflow and $-1\frac{1}{2}$ percent for gross thrust with a deviation about each mean of ±1 percent. The results of an uncertainty analysis are present for both parameters at each simulated flight condition.

INTRODUCTION

An airflow and thrust calibration of an F100 engine, S/N P680059, was undertaken at the NASA Lewis Research Center as part of a program to study airframe - propulsion-system-integration losses in turbofan-powered high-performance aircraft. The calibration, conducted in an altitude test chamber, was coordinated with a flight test program at the NASA Dryden Flight Research Center.

Wind tunnel to flight comparisons have been plagued by the inability of wind tunnel simulation to accurately assess propulsion system component drag (inlet, boattail, etc.) on high-performance aircraft of the type used in flight tests (ref. 1). Engine performance data during flight are normally computed from only a few simple measurements by means of a computer deck supplied by the engine manufacturer. The data obtained at Lewis were compared with values for an average engine from a Pratt & Whitney in-flight

thrust deck (ref. 2) to determine to what extent the differences could be applied to the flight test engine.

The Lewis tests (all steady state) were conducted with and without thrust augmentation over a range of simulated flight conditions representing those scheduled for the flight test. The range of conditions were flight Mach numbers from 0.8 to 1.4, altitudes from 4020 and 15 240 meters (13 200 to 50 000 ft), and nonstandard-day as well as standard-day inlet temperatures. The prime performance variables were corrected airflow and gross thrust. The effect of a simple but typical inlet distortion was also evaluated.

Test results for all conditions are presented in terms of corrected airflow and gross thrust as functions of corrected fan speed for nonaugmented power and corrected gross thrust as a function of fuel-air ratio for augmented power. Comparisons of measured and predicted data are presented along with an uncertainty analysis for both corrected airflow and gross thrust.

APPARATUS

Engine

The F100 engine, S/N P680059, used in this investigation was classified as an F100 $\left(2\frac{7}{8}\right)$ engine which was essentially an F100 (2) configuration with an improved stability fan module and supervisory control logic changes. The control logic changes were made to maintain fan surge margin with engine deterioration and to provide burner pressure bias on the nozzle area setting. The basic F100 engine, shown schematically in figure 1 along with instrument stations, is a 111-kilonewton (25 000-lbf) thrust class Pratt & Whitney engine. It is a low-bypass, high-compression-ratio twin-spool turbofan with a mixed-flow augmentor. A more complete description of the engine and its various models can be found in references 3 to 5.

A unified fuel control handled the primary and some secondary controlling functions, and the engine electronic control (EEC) provided fine trim for the engine. One of the signals to the engine control, flight Mach number, was input at the facility using a Mach number simulator. This device replaced the aircraft Mach number signal allowing the desired input to be dialed into the control. In flight inlet-engine stability is protected during supersonic operation by the EEC based on this Mach number signal. The control accomplishes this by maintaining a minimum total fan airflow for supersonic flight operation.

Facility

The engine installation, a conventional direct connect type, is shown in figure 2 in

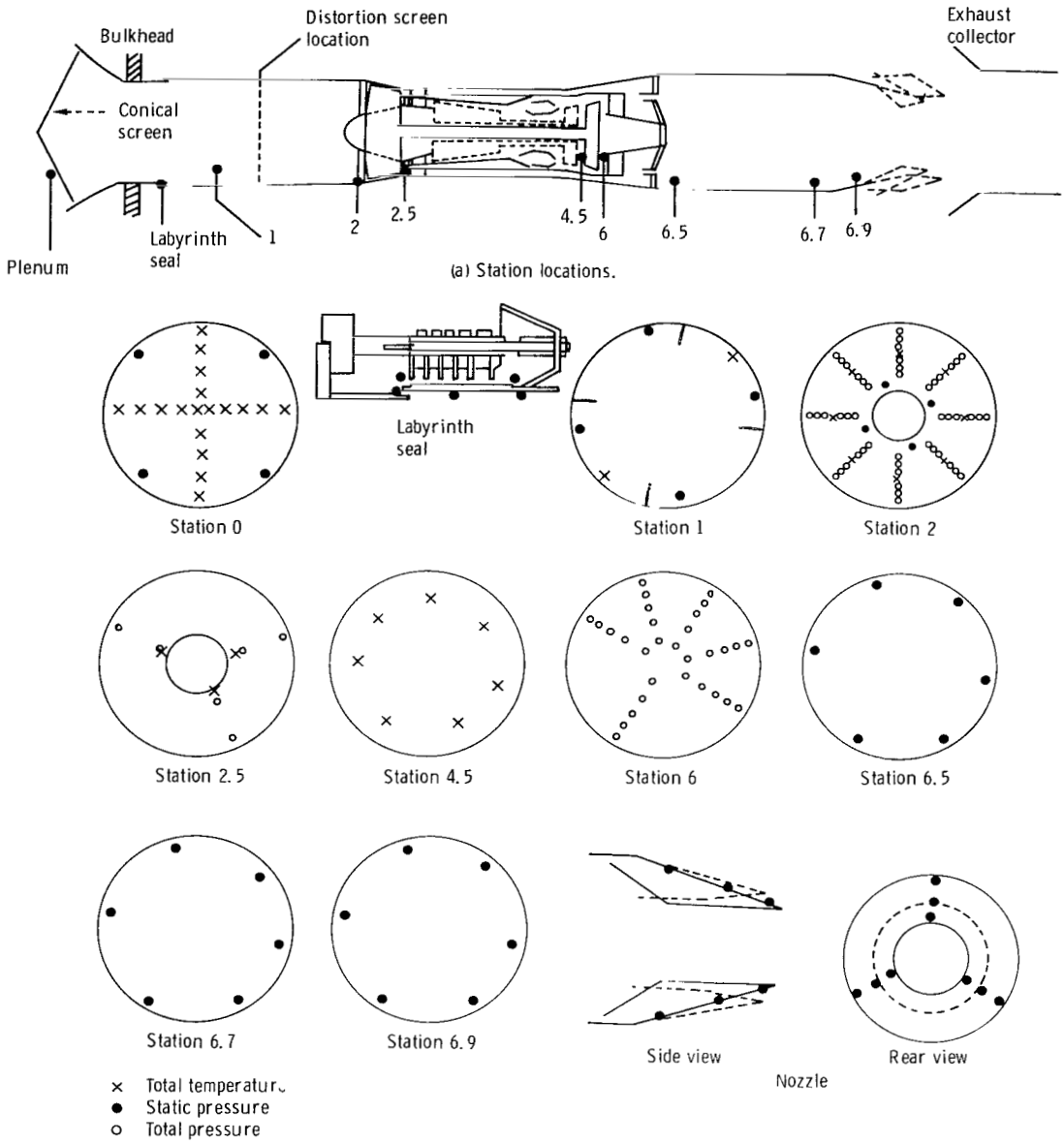

Figure 1. - Engine instrumentation.

the altitude test chamber. The engine was hung from a mounting structure which was attached to a thrust bed. The thrust bed, in turn, was suspended by four flexure rods attached to the chamber supports and was free to move except as restrained by a dual load-cell system that allowed the thrust bed to be preloaded.

The chamber included a forward bulkhead, which separated the inlet plenum (5.5 m (18 ft) diam) from the test chamber (7.3 m (24 ft) diam). Air of the desired temperature and pressure flowed from the plenum through the bellmouth to the inlet duct (fig.

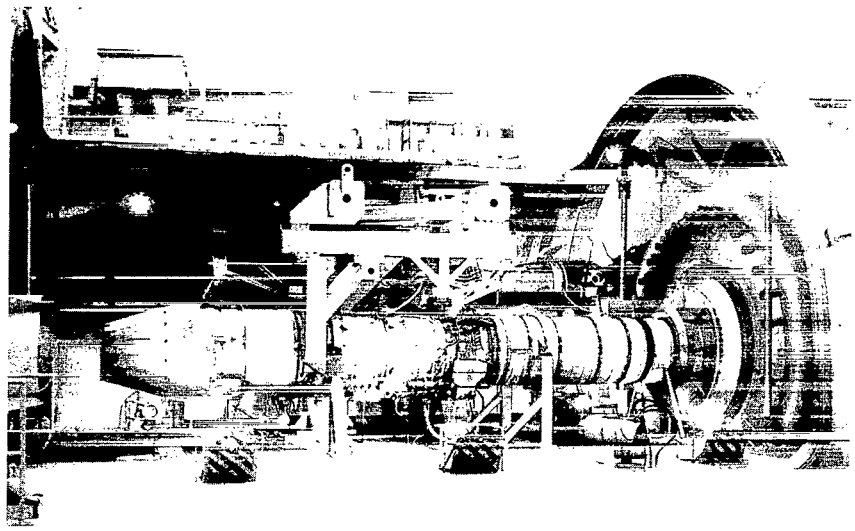

Figure 2. - Altitude test chamber. (F100, S/N P680059, installation.)

1(a)). A labyrinth seal, shown schematically in figure 1(b), was used to isolate the inlet ducting from the bellmouth and bulkhead. The inlet ducting, in turn, was mated to the engine through an inflatable seal that minimized the loading on the engine front flange.

Engine exhaust gases were captured by a collector, which extended through the rear bulkhead, thereby minimizing the possibility of exhaust gas recirculation in the test chamber.

Distortion Screen

An engine inlet total-pressure distortion was produced by the screen pictured in figure 3 and located as shown in figure 1(a), 0.73 meter (2.39 ft) from the engine inlet flange. The screen (an F100-PW-100 Engine Table IIA Distortion Screen, Part No. RA236D-5-1F) had been used to simulate the engine inlet profile at maximum power for a flight Mach number of 0.6 at an altitude of 3050 meters (10 000 ft). The distortion pattern produced by this screen at intermediate power for one test condition is shown in figure 4. The pattern as well as the distortion factor of approximately 14 percent was determined using the technique described in reference 6. The distortion factor was based on the ratio of difference between the maximum and minimum total pressure and the average total pressure.

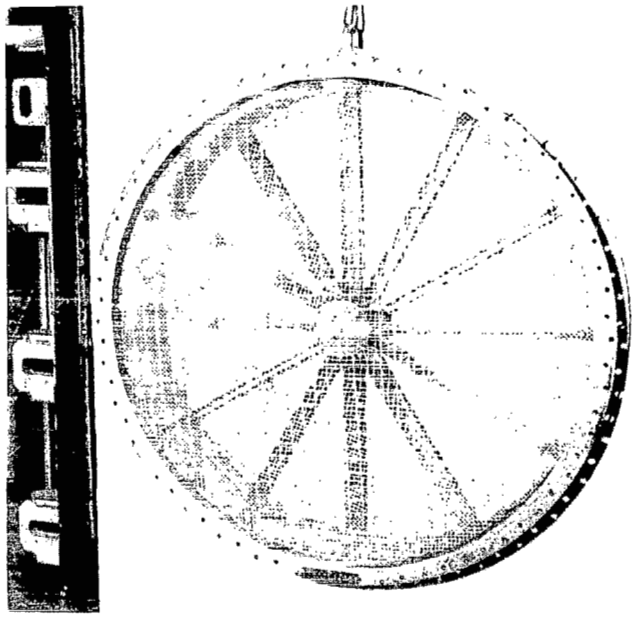

Figure 3. - Distortion screen 5-1F (view looking downstream).

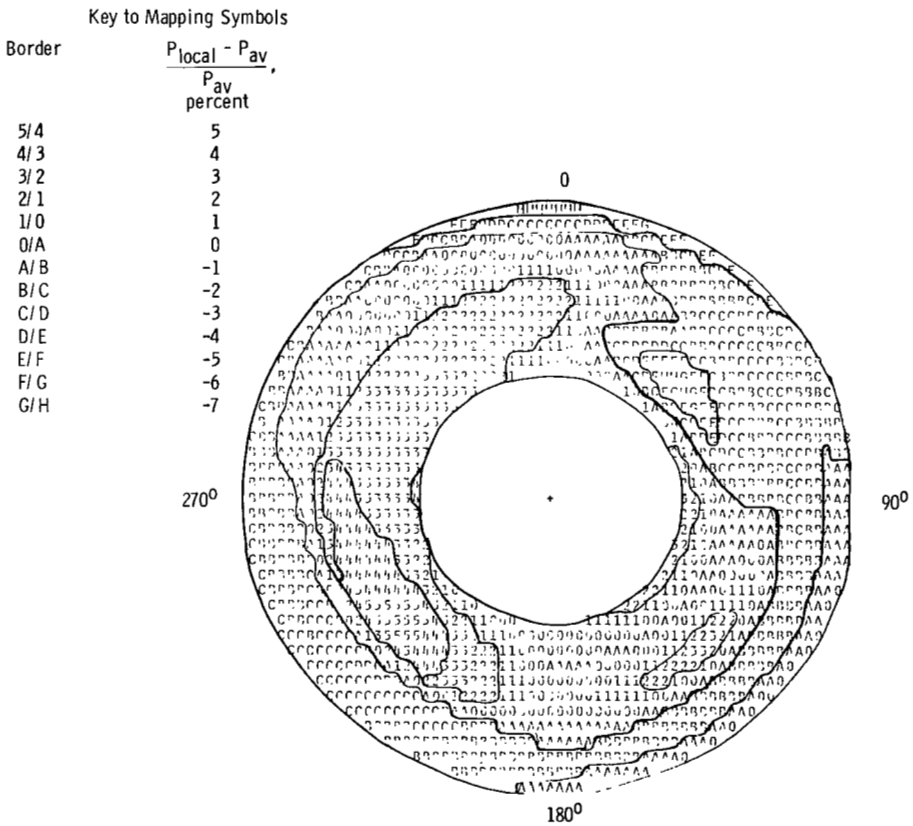

Figure 4. - Distortion pattern produced by screen RA236D-5-1F at the engine inlet for a flight Mach number of 0.8 and an altitude of 4020 meters (13 200 ft); intermediate power.

Instrumentation

Only flight qualified steady-state instrumentation was mounted in the engine; facility instrumentation was used outside the engine. The amount of the instrumentation was minimized to include only those measurements considered necessary for setting test conditions, measuring airflow and gross thrust, and monitoring engine health. The locations of the majority of the instruments are shown schematically in figure 1. (See appendix A for a list of symbols and their definitions.) Not illustrated are fuel flowmeters, both facility and engine mounted, fan and compressor speed instruments, position indicators, accelerometers, and the 106.8-kilonewton (24 000-lbf) load cells.

The steady-state pressures (typical rakes shown in fig. 5) were recorded on nine scanivalves with the exception of the pressures at station 2. These pressures were measured using individual absolute transducers, which were part of the engine inlet rake from the flight program. A detailed description of this rake can be found in reference 7. In two locations, the fan inlet and the compressor inlet, high-response transducers were actually used, but merely as stall indicators. Chromel-Alumel thermocouples, referenced to a 339 K (610° R) oven, were used throughout the installation.

Instrument and system errors, in addition to the equations used to calculate airflow and gross thrust and an uncertainty analysis for airflow and gross thrust, are presented in appendix B.

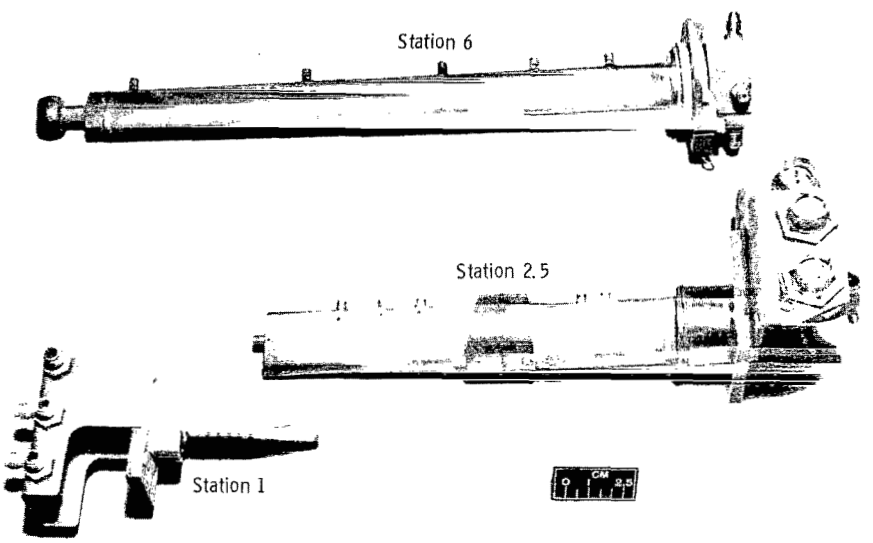

Figure 5. - Typical total pressure rakes.

TEST PROCEDURES

Engine Conditions

Engine inlet pressure and temperature and exhaust pressures were determined by the flight Mach numbers, altitudes, and inlet recovery factors specified by the Dryden Flight Research Center. Inlet pressure was established using an average total pressure at the engine inlet (station 2). This was true with uniform inlet flow as well as with inlet distortion. The inlet temperature was an average of the thermocouple measurements in the inlet plenum, it being assumed that there was no heat lost between the plenum and engine inlet. The simulated altitude conditions were determined in the test cell using the static pressures on the exterior surface of the nozzle (see fig. 1(b)). In particular, the ring of static pressure taps farthest from the nozzle exit plane were used to set test conditions. A complete list of the simulated flight conditions can be found in table I.

As was previously mentioned in the APPARATUS section, the engine control maintained a minimum total fan airflow for supersonic flight operation. However, for the calibration tests, it was considered necessary to investigate part-power (power setting between idle and maximum nonaugmented power) operation while simulating supersonic flight. This was accomplished by dialing a subsonic Mach number into the Mach number simulator, which resulted in the removal of the airflow lockout function and allowed part-power scheduling of the engine control power lever. Test conditions were maintained at simulated supersonic flight pressures and temperatures.

TABLE I. - SIMULATED FLIGHT CONDITIONS

Simulated flight condition	Mach number, M_0	Altitude		Inlet pressure, $P_{t,2}$		Inlet temperature, $T_{t,2}$		Ambient pressure, P_{amb}		Reynolds number index, RNI	Inlet flow
		m	ft	kPa	psia	K	°R	kPa	psia		
1	0.8	4 020	13 200	92.7	13.44	296	532	61.4	8.91	0.89	Uniform
2	.8	↓	↓	↓	↓	284	511	↓	↓	.93	Uniform
3	.8	↓	↓	↓	↓	313	563	↓	↓	.83	Uniform
4	(a)	↓	↓	↓	↓	296	532	↓	↓	.89	Nonuniform
5	.9	7 380	24 200	64.5	9.36	281	505	39.0	5.65	.66	Uniform
6	1.2	12 100	39 700	45.4	6.58	279	502	19.0	2.76	.46	↓
7	1.2	12 700	39 700	45.4	6.58	294	530	19.0	2.76	.45	
8	1.4	15 240	50 000	36.1	5.24	301	542	11.6	1.68	.34	

[a]Ram pressure ratio, $P_{t,2}/P_{amb}$, 1.51.

Nonstandard Day and Inlet Distortion

The effects of nonstandard-day test conditions were evaluated at a ram pressure ratio of 1.51 (for uniform inlet flow this corresponds to a flight Mach number of 0.8) and an altitude of 4020 meters (13 200 ft) over a range of temperatures. Also included was the evaluation of the effects of inlet-flow distortion at this condition. This flight Mach number-altitude was chosen because instrument accuracies were judged best at the relatively high pressure levels. This considered necessary because small differences were expected.

Calculation Program

The Pratt & Whitney In-Flight Thrust Computing Deck (ref. 2) was used to compute gross thrust, which was compared with measured gross thrust. The only program modification was the substitution of measured nozzle area ratios. All inputs were provided from measured data with the exception of an augmentor inlet total temperature. No thermocouples were available for this measurement. The baseline corrected airflow data in the Pratt & Whitney program was curve fit by Dryden and formed a basis of comparison for the measured corrected airflow data. The baseline data are defined as those data which excluded corrections for such factors as Reynolds number effects, guide-vane angle variation, inlet distortion, and a term referred to as an "airflow correction from deck to engine" (ref. 2). The curve fits required only measured corrected fan speed and engine pressure ratio as input to determine corrected airflow.

RESULTS AND DISCUSSION

Airflow and thrust calibration tests were conducted with and without augmentation for a variety of simulated flight conditions with emphasis on the transonic regime. Results from these tests are presented in figures 6 to 14 in terms of (1) corrected airflow and corrected gross thrust as functions of corrected fan speed for nonaugmented power and (2) corrected gross thrust as a function of fuel-air ratio for augmented power. Comparisons of these measured results with calculated data are displayed in figures 15 and 16, and the results of an uncertainty analysis for both measured corrected airflow and gross thrust are shown in table II. The design corrected airflow used to normalize the data was 98.4 kilograms per second (217 lbm/sec); the nominal corrected gross thrust was arbitrarily chosen as 111 kilonewtons (25 000 lbf).

Standard Day

Corrected airflow as a function of corrected fan speed over a range of flight Mach numbers and altitudes is presented in figure 6. A range of corrected fan speeds from part power, approximately 6000 rpm, to intermediate power (maximum nonaugmented power setting was investigated with all data collapsing into a single curve with little scatter. Data at a Reynolds number index of 0.34 showed no apparent shift from the other three test conditions, which were at or above a Reynolds number index of 0.5.

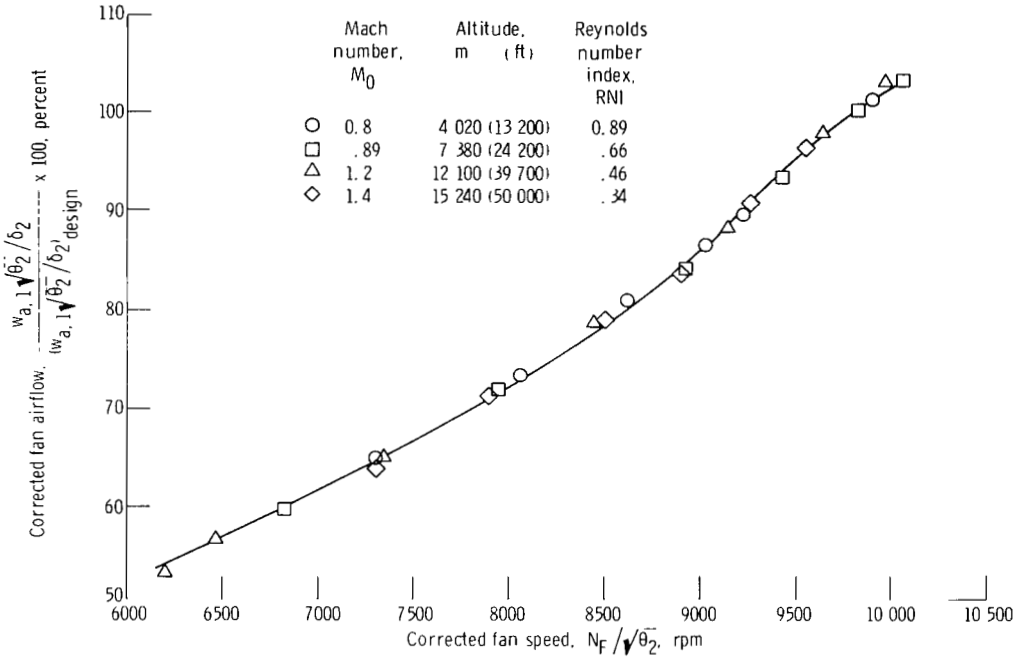

Figure 6. - Corrected airflow as function of corrected fan speed.

The presentation of corrected gross thrust as a function of corrected fan speed (fig. 7) for a range of Mach numbers, altitudes, and Reynolds number indexes contrasts with the airflow curve of figure 6 in that each test condition resulted in a distinct set of data. Over the range of parameters investigated, corrected gross thrust increased as the simulated flight conditions were changed from the lowest to the highest flight Mach number-altitude combination.

The corrected gross thrust data for augmented power (fig. 8) are plotted as a ratio of corrected gross thrust at selected augmentor power lever angles to the corrected gross thrust at intermediate power for the same test condition. Except for minimum and maximum augmentation, these data were recorded at a power lever angle corresponding to the midpoint of each augmentor segment. A few of the upper segments were not inves-

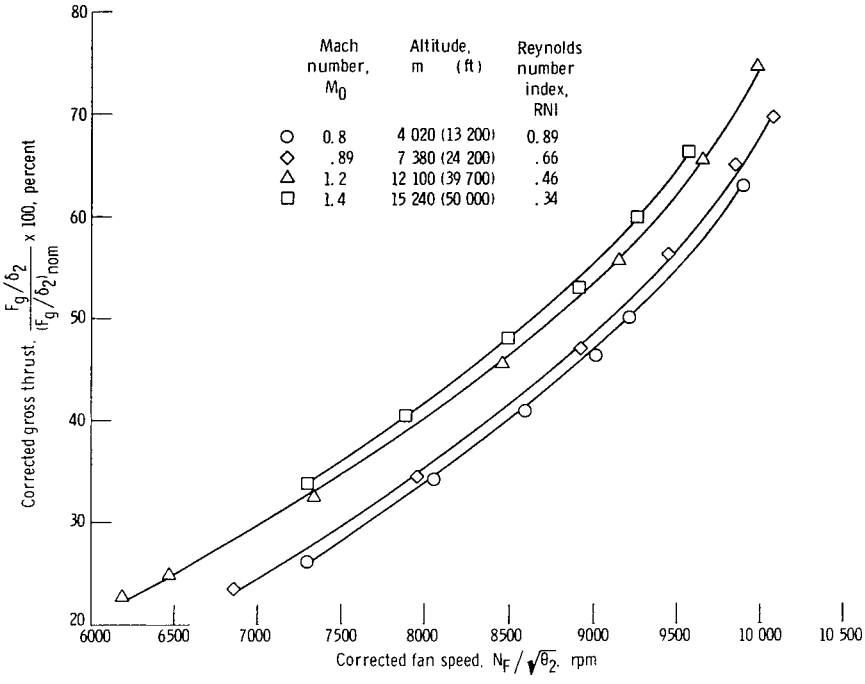

Figure 7. - Corrected gross thrust as function of corrected fan speed.

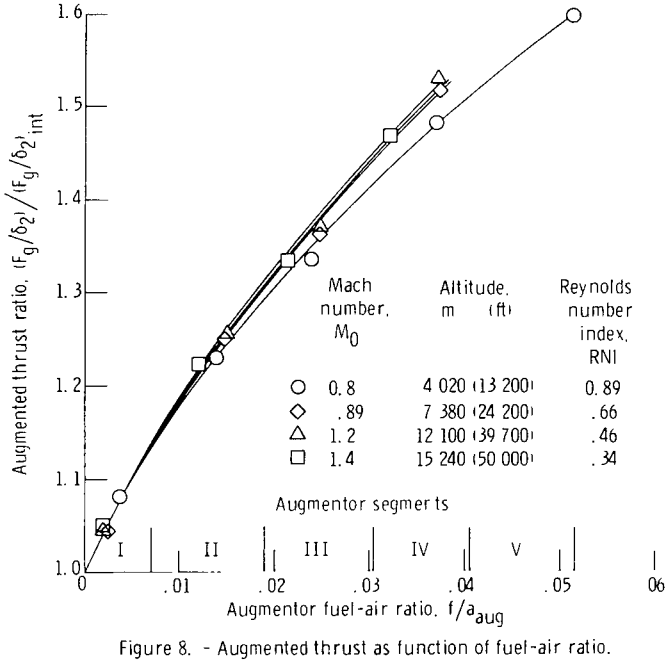

Figure 8. - Augmented thrust as function of fuel-air ratio.

tigated because of a restriction in the facility fuel supply line. The augmentor fuel-air ratio is the ratio of the augmentor fuel flow to the unburnt air - that is, the air associated with the oxygen consumed in the primary combustor was subtracted from the total airflow (see appendix B). This is the method used previously in reference 8.

Generally, the trend observed for nonaugmented power (fig. 7) of an increase in corrected gross thrust resulting from an increase in flight Mach number and altitude followed for augmented power. A secondary observation is that, in general, the data scatter, even with the sensitive augmented thrust ratio, was small enough that each set of data could be separated to form individual curves.

Nonstandard Day and Inlet Distortion

Inlet temperature variation. - An inlet temperature variation from 284 to 313 K (511° to 563° R) was accomplished at the primary test condition. Corrected airflow (fig. 9) and corrected gross thrust (fig. 10) are plotted against corrected fan speed for nonaugmented power, and corrected gross thrust is plotted as an augmented thrust ratio versus fuel-air ratio for augmented power (fig. 11). Without augmentation the nonstandard-day inlet temperatures permitted an extension of both airflow and thrust curves to higher and lower corrected fan speeds. Otherwise, little or no difference was evident on either plot (figs. 9 or 10) with inlet temperature variation. Gross thrust during augmentation (fig. 11) is plotted similarly to the data previously presented for standard-day performance in figure 8. Generally, the augmentation data agreed with standard-day performance, although there was slightly more data scatter.

Inlet flow distortion. - The corrected airflow and corrected gross thrust data for the nonuniform inlet condition are plotted in figures 12 to 14 in a fashion similar to the previously presented data. The screen distortion, which resulted in approximately a 14-percent distortion factor (see ref. 6) at intermediate power, was insufficient to cause a difference in corrected airflow and gross thrust between uniform and nonuniform inlet conditions within the accuracy of the data.

Data Comparisons and Accuracies

A primary objective of the calibration tests, besides providing data for the flight program, was to compare measured results with calculated data - in this case those from an in-flight thrust computing program (ref. 2). It follows that the accuracy of the measured data is also of prime importance. The results of the comparison between measured and calculated data and an uncertainty analysis of the measured data are presented herein.

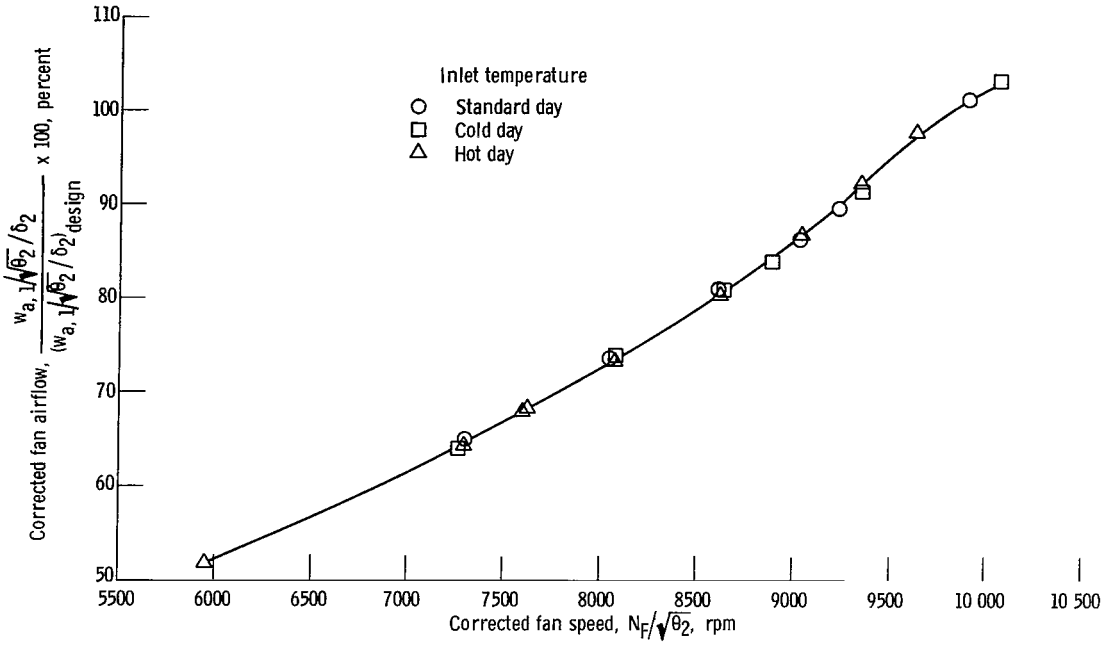

Figure 9. - Corrected airflow as function of corrected fan speed over range of inlet temperatures. Mach number, 0.8; altitude, 4020 meters (13 200 ft).

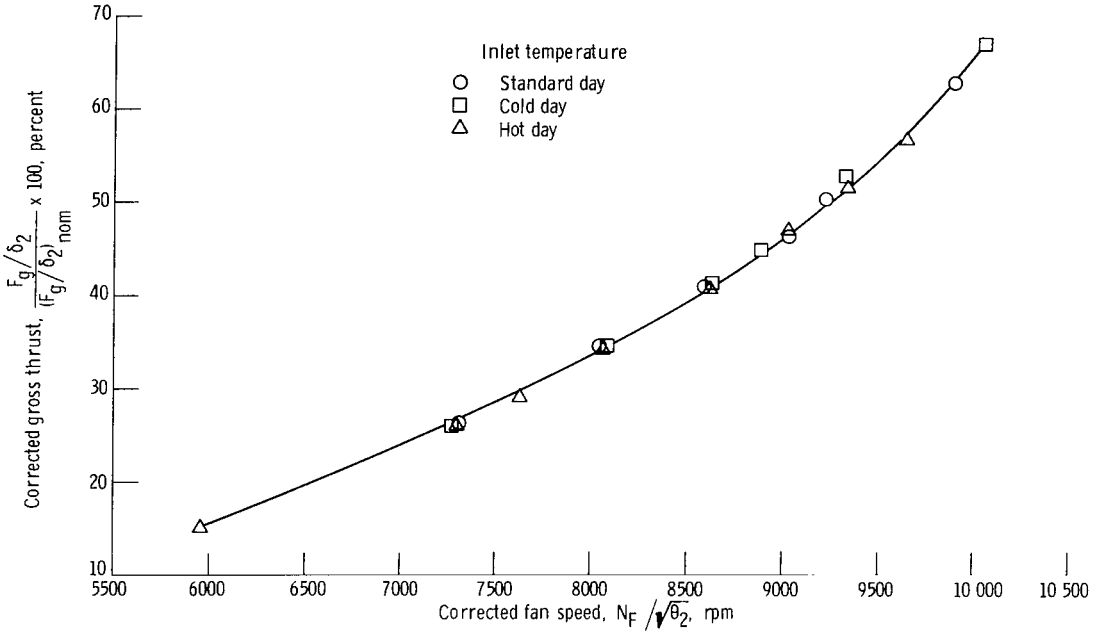

Figure 10. - Corrected gross thrust as function of corrected fan speed over range of inlet temperatures. Mach number, 0.8; altitude, 4020 meters (13 200 ft).

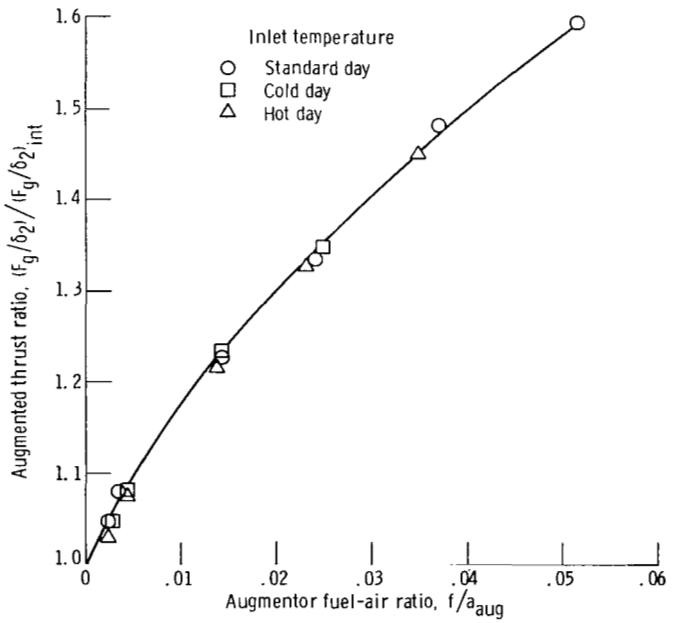

Figure 11. - Augmented thrust as function of augmentor fuel-air ratio over range of inlet temperatures. Mach number, 0.8; altitude, 4020 meters (13 200 ft).

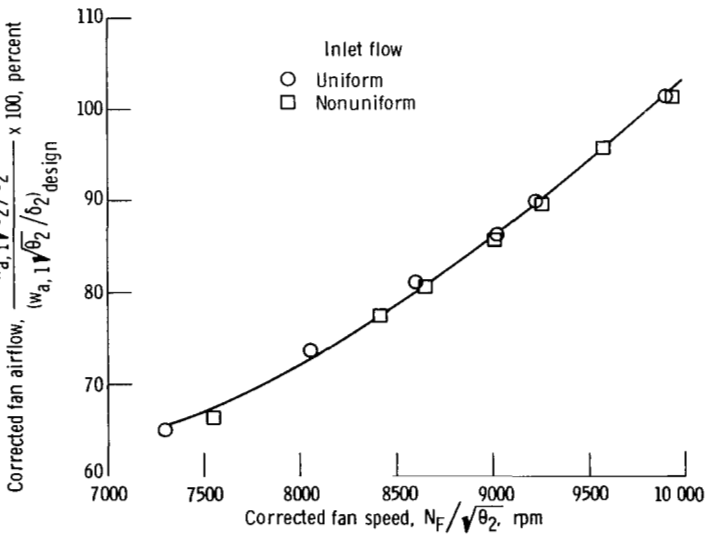

Figure 12. - Corrected airflow as function of corrected fan speed with and without uniform inlet flow. Ram pressure ratio, 1.51; altitude, 4020 meters (13 200 ft).

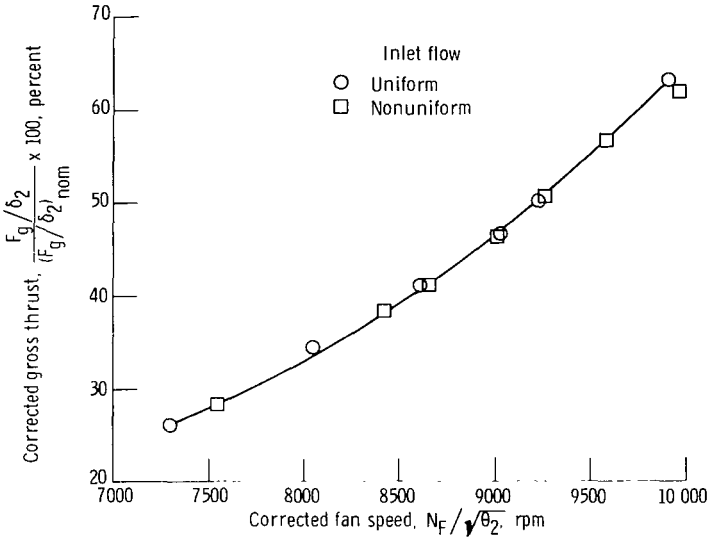

Figure 13. - Corrected gross thrust as function of corrected fan speed with and without uniform inlet flow. Ram pressure ratio, 1.51; altitude, 4020 meters (13 200 ft).

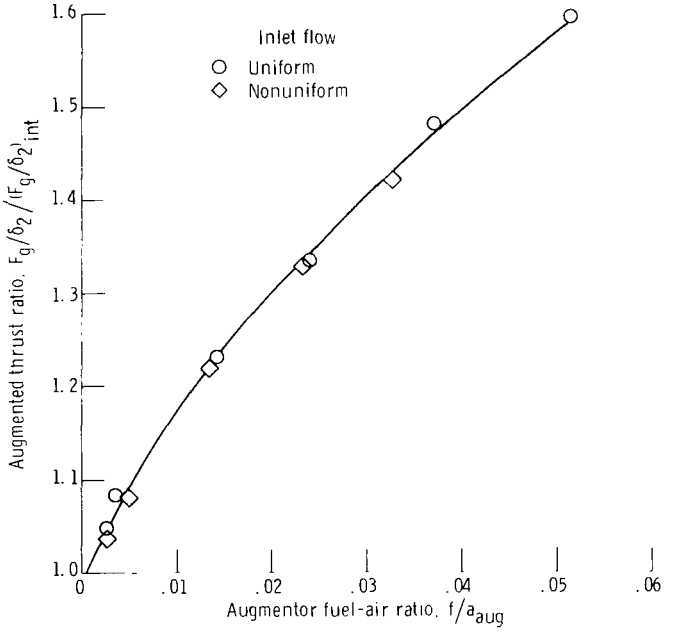

Figure 14. - Augmented thrust as function of augmentor fuel-air ratio with and without uniform inlet flow. Ram pressure ratio, 1.51; altitude, 4020 meters (13 200 ft).

Data comparisons. - In figures 15 and 16 corrected airflow and gross thrust (as measured) are compared with the results from the calculation program. Included in these plots are the data at a flight Mach number of 1.2, an altitude of 12 100 meters (39 700 ft), and a hot-day inlet temperature which were not previously presented. The deviation of corrected airflow (fig. 15) is the difference between measured and calculated values and is plotted against measured corrected airflow. Generally, all the data fell within a band of ±1 percent of the mean with the mean of the measured data 1 percent greater than that of the calculated data. The only exceptions for all the data were in the region of 75 to 80 percent of design corrected airflow where differences between measured and calculated data of up to $2\frac{1}{2}$ percent were evident. In this region the corrected airflow and fan-speed relation was particularly sensitive. The inlet distortion data are also of interest because of the somewhat greater scatter than the uniform flow data. As was previously noted, the calculated data excluded corrections for such factors as inlet distortion. Likewise, it has been stated previously that these distortion data differed little from the uniform flow data (fig. 13). This observation is not necessarily contradicted by the data presented in figure 15. The differences between the two sets of data

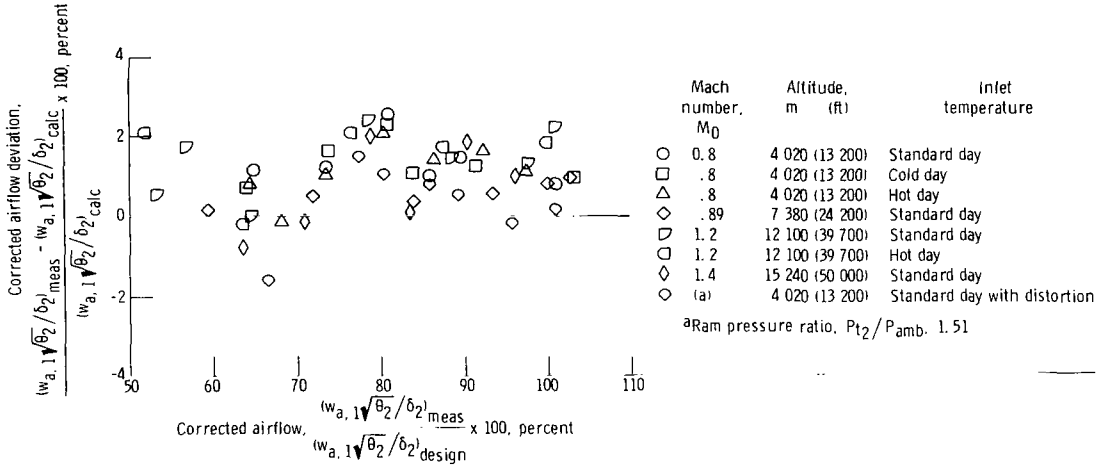

Figure 15. - Corrected airflow comparison.

are within the uncertainty bands of the measured data and the calculated values.

It should be noted that greater airflow uncertainties existed at a flight Mach number of 1.4 and 15 240 meters (50 000 ft) as shown in table II. However, only at the lower corrected airflow at this condition are the data outside the band of ±1 percent.

The comparison with calculated gross thrust is displayed in figure 16 for all test conditions. Gross thrust rather than corrected gross thrust is presented because the

TABLE II. - MEASUREMENT UNCERTAINTIES

Simulated flight condition number	Power lever angle[a]	Uncertainties, percent of measurement	
		Corrected airflow	Gross thrust
1	I	±0.6	±0.4
	M	----	±.2
2	I	±.6	±.4
	M	----	±.3
3	I	±.6	±.4
	M	----	±.3
4	I	±.6	±.4
	M	----	±.3
5	I	±.7	±.5
	M	----	±.3
6	I	±.8	±.6
	M	----	±.4
7	I	±.8	±.7
	M	----	±.5
8	I	±1.0	±.9
	M	----	±.6

[a]I denotes intermediate power; M denotes maximum attainable power lever angle.

normalization of both measured and calculated results adds nothing to the interpretation of the data. The range of gross thrust from part power to maximum augmentation includes data from approximately 10 to 90 percent of the nominal gross thrust. The mean of measured gross thrust data was $1\frac{1}{2}$ percent less than the calculated gross thrust with the vast majority of the data within a band of ±1 percent about the mean. The general shape of the plotted results, where the data scatter is large at the lower thrust levels and smaller at the higher levels, is similar to at least one other example using a version of the calculation program (ref. 9). This would suggest that errors in measuring thrust are more or less fixed, and, therefore, as thrust increases, the errors are proportionally of less influence. This would account for errors outside the band of the majority of the data below 15 percent gross thrust. Two other areas of interest where the data are slightly beyond the nominal tolerance band of ±1 percent are at the intermediate power point and the minimum augmentation region. At both conditions the nozzle throat area was programmed for its initial movements. Difficulties in the measuring nozzle throat area may influence the calculated data to a large extent. Gross thrust data for inlet distortion are not presented because it appeared that the introduction of distortion factors into the calculation program had no influence on thrust.

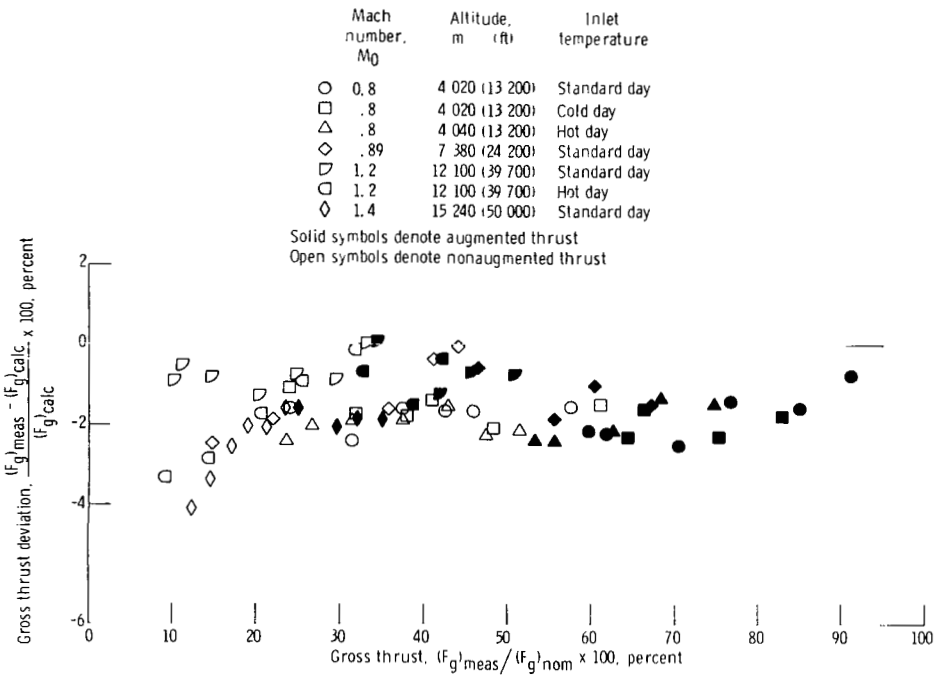

Figure 16. - Thrust comparison.

Measured data uncertainty. - The results of an uncertainty analysis for the measured data at selected test conditions are listed in table II for corrected airflow and gross thrust. These uncertainties were calculated using the instrument inaccuracies and the uncertainty equations presented in appendix B. At intermediate power the corrected airflow and gross thrust uncertainties for the majority of the data were less than 1 percent. At the maximum power setting for each condition, gross thrust uncertainties were 0.6 percent or less. The decrease in uncertainties from those at intermediate power was anticipated since the calculated parameters (e.g., inlet momentum) were fixed while only load cell measurements - inherently more accurate - changed.

SUMMARY OF RESULTS

An airflow and thrust calibration was conducted with an F100 engine, S/N P680059, for a variety of simulated flight conditions. The principal results of this calibration were

1. All corrected airflow data at Reynolds number indexes of 0.5 and greater generalized into one curve against corrected fan speed. In addition, no shift in the correla-

tion was apparent for data at a Reynolds number index less than 0.5.

2. With and without augmentation, corrected gross thrust increased as simulated flight Mach number and altitude increased.

3. Over a range of inlet temperatures at constant Mach number, corrected airflow and gross thrust correlated with corrected fan speed for nonaugmented power, and corrected gross thrust correlated with fuel-air ratio for augmented power.

4. Overall agreement between measured and calculated data using a Pratt & Whitney computer deck was 1 percent for corrected airflow and $-1\frac{1}{2}$ percent for gross thrust with a deviation about each mean of ±1 percent. The measured data uncertainties for the majority of the data were less than 1 percent for corrected airflow and gross thrust at intermediate power and 0.6 percent or less for gross thrust at the maximum attainable power for each test condition.

5. No change was evident in corrected airflow and corrected gross thrust with an inlet distortion factor of 14 percent.

Lewis Research Center,
National Aeronautics and Space Administration,
Cleveland, Ohio, October 31, 1977,
505-05.

APPENDIX A

SYMBOLS

A	area, cm^2
DP	differential pressure, kPa
F_{cowl}	force present if pressure on exterior surface of nozzle is not equal to test cell pressure, N
F_{defl}	force due to deflection of thrust bed plus friction in bed, N
F_g	gross thrust, N
F_m	load cell measurement, N
F_p	preload, N
F_{seal}	force on labyrinth seal flange, N
F_{tare}	force caused by air flowing through labyrinth seal, N
f/a	fuel to air ratio
g_c	units constant, $kg \cdot m/(N \cdot sec^2)$
M	Mach number
N	rotor speed, rpm
P	pressure, kPa
R	gas constant, $J/(kg \cdot K)$
RNI	Reynolds number index, $\delta/(\mu/\mu_{std})\sqrt{\theta}$
T	temperature, K
V	velocity, m/sec
w	mass flow rate, kg/sec
γ	ratio of specific heats
Δ	error
δ	ratio of total pressure to standard sea-level static pressure
θ	ratio of total temperature to standard sea-level static temperature
μ	absolute viscosity, $kg/(m \cdot sec)$

Subscripts:

a	air
amb	ambient
aug	augmentor
av	average
calc	calculated value from Pratt & Whitney computer deck (ref. 2)
cowl	exterior engine exhaust nozzle surface
design	design point
e	engine
F	fan
f	fuel
int	intermediate throttle setting
meas	measured value
nom	nominal value
pl	plenum
s	static
seal	seal location
std	standard sea level static conditions
t	total
0	station 0, or free stream
1	station 1, flow measuring station
2	station 2, engine inlet
2.5	station 2.5, fan exit
4.5	station 4.5, fan-turbine inlet
6	station 6, fan-turbine exit
6.5	station 6.5, augmentor liner
6.7	station 6.7, augmentor liner
6.9	station 6.9, augmentor liner

APPENDIX B

METHODS OF CALCULATION

Measurement Uncertainties

Airflow systematic error. - Total corrected airflow at the engine inlet (station 2) was measured by an area integration of the flow at station 1 using the following equation:

$$\frac{w_{a,1}\sqrt{\theta_2}}{\delta_2} = \sqrt{\frac{2g_c}{RT_{std}}\left(\frac{\gamma}{\gamma - 1}\right)}\left(\frac{A_1 P_{t,1} P_{std}}{P_{t,2}}\right)\left(\frac{P_{s,1}}{P_{t,1}}\right)^{1/\gamma}\sqrt{1 - \left(\frac{P_{s,1}}{P_{t,1}}\right)^{(\gamma-1)/\gamma}}$$

The airflow systematic error was found from the weighted root-sum-square combination of the instrumentation error limits (Taylor series expansion of the airflow equation) as follows:

$$\frac{\Delta\left(\frac{w_{a,1}\sqrt{\theta_2}}{\delta_2}\right)}{\frac{w_{a,1}\sqrt{\theta_2}}{\delta_2}} = \left[\left(\frac{\Delta A_1}{A_1}\right)^2 + \left(\frac{\Delta P_{t,2}}{P_{t,2}}\right)^2 + C_1^2\left(\frac{\Delta DP_1}{DP_1}\right)^2 + (1 - C_1)^2\left(\frac{\Delta P_{t,1}}{P_{t,1}}\right)^2\right]^{1/2}$$

where

$$C_1 = \frac{\frac{1}{\gamma}\left(\frac{P_{t,1}}{P_{s,1}} - 1\right)\left[\frac{\gamma + 1}{2} - \left(\frac{P_{t,1}}{P_{s,1}}\right)^{(\gamma-1)/\gamma}\right]}{\left(\frac{P_{t,1}}{P_{s,1}}\right)^{(\gamma-1)/\gamma} - 1}$$

Neither the $P_{t,1}$ nor $P_{s,1}$ error term occur in the preceding equation because their common error terms arise from the scanivalve measuring system. Independence of error terms is required for a root sum square combination - a condition more nearly satisfied by the differential pressure DP_1 and $P_{t,1}$.

Gross thrust systematic error. - The gross thrust was determined as follows:

$$F_g = F_m - F_p + F_{defl} + F_{tare} + F_1 + F_{seal} - F_{cowl}$$

The momentum term F_1 included an area integration at station 1 using the following equation:

$$F_1 = A_1\left[P_{s,1}\left(\gamma M_1^2 + 1\right) - P_{amb}\right]$$

The gross thrust systematic error was found from the weighted root-sum-square combination of the instrumentation error limits:

$$\Delta F_g = \Big[(\Delta F_m)^2 + (\Delta F_p)^2 + (\Delta F_{defl})^2 + (\Delta F_{tare})^2 + A_1^2(\Delta P_{amb})^2 + C_2^2(\Delta A_1)^2$$

$$+ C_3^2(\Delta P_{s,1})^2 + C_4^2(\Delta DP_1)^2 + (DP_{seal})^2(\Delta A_{seal})^2 + A_{seal}^2(\Delta DP_{seal})^2$$

$$+ (DP_{cowl})^2(\Delta A_{cowl})^2 + A_{cowl}^2(\Delta DP_{cowl})^2\Big]^{1/2}$$

where

$$C_2 = \frac{F_1}{A_1}; \qquad C_3 = A_1\left[\gamma M_1^2 + 1 - 2\,\frac{\frac{P_{t,1}}{P_{s,1}} - 1}{\left(\frac{P_{t,1}}{P_{s,1}}\right)^{1/\gamma}}\right]$$

$$C_4 = \frac{2A_1}{\left(\frac{P_{t,1}}{P_{s,1}}\right)^{1/\gamma}}$$

Instrumentation errors. - The following values were obtained from data compiled during an investigation of the instrumentation and recording systems. In general, the parameters were taken as independent of each other, and the delta values represented their limit of error.

Item	System Total Error
ΔP	0.3 kPa (0.05 psia)
ΔDP	greater of 0.03 kPa (0.005 psia) or 0.5 percent
ΔT_t	2 K (3° R)
ΔA	0.5 cm^2 (0.1 in^2)
ΔF_m	45 N (10 lbf)
ΔF_p	45 N (10 lbf)
ΔF_{defl}	70 N (15 lbf)
ΔF_{tare}	70 N (15 lbf)

Augmentor Fuel-Air Ratio

The augmentor fuel-air ratio was defined as the ratio of the augmentor fuel flow to the unburned air entering the augmentor. Engine combustion efficiency was assumed to be 100 percent.

$$\left(\frac{f}{a}\right)_{aug} = \frac{w_{f,t} - w_{f,e}}{w_{a,1} - \frac{w_{f,e}}{0.06728}}$$

where 0.06728 is the stoichiometric fuel-air ratio of the JP-4 fuel used.

REFERENCES

1. Bellman, Donald R.; Burcham, Frank W., Jr.; and Taillon, Norman V.: Techniques for the Evaluation of Air-Breathing Propulsion Systems in Full-Scale Flight. NASA TM X-68305, 1972.

2. F100 (3) In-Flight Thrust Calculation Deck. CCD 1088-2.0, Pratt & Whitney Aircraft, March 31, 1975.

3. Sams, H.: F-15 Propulsion System Design and Development. AIAA Paper 75-1042, Aug. 1975.

4. Staley, E. J.: F-15 Propulsion Flight Testing Experience. AIAA Paper 75-1052, Aug. 1975.

5. Taylor, John W. R., ed.: Jane's All the World's Aircraft 1975-1976. Franklin Watts Inc., 1975.

6. Dicus, John H.: Fortran Program to Generate Engine Inlet Flow Contour Maps and Distortion Parameters. NASA TM X-2967, 1974.

7. Farr, A. Pike: Evaluation of F-15 Inlet Dynamic Distortion. AIAA Paper 73-784, Aug. 1973.

8. McAulay, John E.; and Abdelwahab, Mahmood: Experimental Evaluation of a TF30-P-3 Turbofan Engine in an Altitude Facility: Afterburner Performance and Engine-Afterburner Operating Limits. NASA TN D-6839, 1972.

9. Hatt, F. George; and Hancock, Dain M.: Recent Flight Experience With the F100 Engine in the YF-16. J. Aircr., vol. 12, no. 12, Dec. 1975, pp. 948-953.

1. Report No.	2. Government Accession No.	3. Recipient's Catalog No.
NASA TP-1069		

4. Title and Subtitle
AIRFLOW AND THRUST CALIBRATION OF AN F100 ENGINE, S/N P680059, AT SELECTED FLIGHT CONDITIONS

5. Report Date: April 1978

6. Performing Organization Code:

7. Author(s)
Thomas J. Biesiadny, Douglas Lee, and Jose R. Rodriguez

8. Performing Organization Report No.: E-9257

10. Work Unit No.: 505-05

9. Performing Organization Name and Address
National Aeronautics and Space Administration
Lewis Research Center
Cleveland, Ohio 44135

11. Contract or Grant No.:

13. Type of Report and Period Covered: Technical Paper

12. Sponsoring Agency Name and Address
National Aeronautics and Space Administration
Washington, D. C. 20546

14. Sponsoring Agency Code:

15. Supplementary Notes

16. Abstract

An airflow and thrust calibration of an F100 engine, S/N P680059, was conducted at the NASA Lewis Research Center in coordination with a flight test program at the NASA Dryden Flight Research Center to study airframe-propulsion system integration losses in turbofan-powered high-performance aircraft. The tests were conducted with and without thrust augmentation for a variety of simulated flight conditions with emphasis on the transonic regime. The resulting corrected airflow data generalized into one curve with corrected fan speed while corrected gross thrust increased as simulated flight conditions increased. Overall agreement between measured data and computed results from a Pratt & Whitney Aircraft in-flight thrust deck was 1 percent for corrected airflow and $-1\frac{1}{2}$ percent for gross thrust. The results of an uncertainty analysis are presented for both parameters at each simulated flight condition.

17. Key Words (Suggested by Author(s))	18. Distribution Statement
Turbofan engines Jet propulsion Altitude tests Altitude simulation	Unclassified - unlimited STAR Category 07

19. Security Classif. (of this report)	20. Security Classif. (of this page)	21. No. of Pages	22. Price*
Unclassified	Unclassified	25	A02

* For sale by the National Technical Information Service, Springfield, Virginia 22161

NASA-Langley, 1978

National Aeronautics and Space Administration

Washington, D.C.
20546

Official Business
Penalty for Private Use, $300

THIRD-CLASS BULK RATE

Postage and Fees Paid
National Aeronautics and
Space Administration
NASA-451

1 1 1U,A, 040878 S00903DS
DEPT OF THE AIR FORCE
AF WEAPONS LABORATORY
ATTN: TECHNICAL LIBRARY (SUL)
KIRTLAND AFB NM 87117

NASA

POSTMASTER: If Undeliverable (Section 158 Postal Manual) Do Not Return